




Coupled cluster theory for the ground and excited states of two-dimensional quantum dots

Faruk Salihbegović , Alejandro Gallo , and Andreas Grüneis 

Institute for Theoretical Physics, Vienna University of Technology (TU Wien), A-1040 Vienna, Austria, EU



(Received 12 November 2021; revised 27 January 2022; accepted 22 February 2022; published 8 March 2022)

We present a study of the two-dimensional circular quantum dot model Hamiltonian using a range of quantum chemical *ab initio* methods. Ground and excited state energies are computed on different levels of perturbation theories, including the coupled cluster method. We outline a scheme to compute the required Coulomb integrals in real space and utilize a semianalytic solution to the integral over the Coulomb kernel in the vicinity of the singularity. Furthermore, we show that the remaining basis set incompleteness error for two-dimensional quantum dots scales with the inverse number of virtual orbitals, allowing us to extrapolate to the complete basis set limit energy. By varying the harmonic potential parameter we tune the correlation strength and investigate the predicted ground and excited state energies.

DOI: [10.1103/PhysRevB.105.115111](https://doi.org/10.1103/PhysRevB.105.115111)

I. INTRODUCTION

A quantum dot (QD) is a semiconducting nanocrystal typically embedded in a host semiconductor with a larger band gap such that the excitons of the QD have a de Broglie wavelength comparable to the size of the crystal. The typical size of such a nanocrystal is 2–100 nm and it is made out of roughly a million atoms. In this context, virtually all electrons are tightly bound to the nuclei of the material such that the number of free electrons in a QD ranges typically from 1 to 100. As described by the quantum mechanical theory of solids, the electrons do not get trapped in the real nuclei of the material but instead simply sense a potential well of the QD, thus forming discrete energy levels. These electrons behave as free electrons with a renormalized mass. For example, electrons in the semiconductor GaAs appear to carry a mass of only 7% of the mass of free electrons. QDs are often referred to as artificial atoms because they exhibit similar properties as atoms (level spacing, ionization energy, magnetic moments) albeit on different energy scales.

Due to their tunable optical and electronic properties, QDs are widely used in many practical applications including solar cells, light-emitting diodes, laser technology, as well as biological and biomedical applications [1–7]. The use of QDs as cosmetic hair dyes is the oldest known application, dating back more than 2000 years, when PbS QDs were synthesized using naturally occurring materials like $\text{Ca}(\text{OH})_2$, PbO, and water [8]. Over the past few decades, several ways to synthesize and investigate dynamical properties of QDs with extraordinary high precision have been developed [9]. Consequently, experimental and theoretical research on these nanoparticles has harnessed much attention and insight [6,7,10–33].

The simplest model used in theoretical studies of QDs, which has proven to be adequate, is the harmonic oscillator [34]. In this model, the interaction of the electrons with the surrounding semiconductor material is approximated through the material-specific effective mass of the electrons and a

material-specific relative dielectric constant that screens the Coulomb interaction. In passing we note that a more realistic nanoscale model of QDs can be obtained by an empirical pseudopotential based approach [35,36]. In contrast to other many-body systems, in QDs, the coupling strength of the two-body operator relative to the one-body operator can be freely varied over a wide range of values, thus giving rise to various regimes of interelectronic correlation. The simple expression of the QD model Hamiltonian allows for a straightforward application of many-electron methods that have historically been developed for atoms and crystals. Density functional theory (DFT) using approximate density functionals is computationally extremely efficient and able to account for a large part of the electron correlation. However, its general applicability is often hindered by uncontrolled approximations used for constructing the approximate exchange-correlation functional. Notwithstanding its drawbacks, one-electron theories such as DFT in the Kohn-Sham framework of approximate exchange and correlation (XC) energy functionals [37–40] and the Hartree-Fock (HF) [15,41–50] approximation often achieve a qualitatively correct agreement with experiment. In contrast to DFT calculations, full configuration interaction (FCI) investigations of QDs yield exact results for a given basis set and have been applied to QDs in a number of studies [4,49,51–65]. FCI employs excited Slater determinants to span a many-body wave function space and through exact diagonalization finds a superposition of Slater determinants with the lowest energy. However, since the size of this space grows combinatorially fast with respect to the number of particles and basis functions, FCI is prohibitively computationally expensive. Alternatively, a technique that has been used for QDs thoroughly is quantum Monte Carlo (QMC) [64,66–74]. Here the computational cost grows relatively modestly with the number of electrons and it provides highly accurate ground state energies. Moreover, there is the possibility to use the nodal structure of the ground state trial wave function to impose restrictions on the solutions. In this way, excited states can be calculated as well even if calculations on general

excited states are not straightforward. Coupled cluster (CC) theory combines accuracy with feasibility, being numerically less expensive than FCI while having size consistency by construction and providing ground state and excited state energies with an accuracy that is comparable to quantum QMC calculations [75,76]. Second-order Møller-Plesset perturbation theory (MP2) and coupled cluster singles doubles (CCSD) have been shown to be useful approaches to calculate atomic, molecular, and solid-state properties [77–82]. They have also been used to study QD Hamiltonians in a number of studies [75,76,83–85]. Via the equation of motion (EOM) formalism, CC theory can also be applied to excited states [86], and was already applied to atoms, molecules, and recently even solids [77,87–89] and quantum plasmons and excitons [90]. Here we seek to apply equation of motion CCSD (EE-EOM-CCSD) theory to study excited states in two-dimensional QDs [91,92]. To this end we employ an implementation of EE-EOM-CCSD that was recently used to investigate defects in solids employing *ab initio* Hamiltonians [89].

This paper is organized as follows. In Secs. II A and II B we introduce the Hamiltonian of the QD and its solutions for the single particle case. In Sec. II D we present a way to calculate the Coulomb matrix elements needed for the many-electron Hamiltonian by employing analytical solutions for the integral over the Coulomb kernel near the singularity in a 4D hypercube. Further in Sec. II C we provide an overview of the CCSD and EE-EOM-CCSD approaches used to calculate the ground state and excited state energies. In Secs. III A and III B we present the results of the CCSD and EE-EOM-CCSD calculations for the ground state and excited states energies of QDs in different confinement regimes for 2, 6, and 12 electrons and compare them to other findings from the literature.

II. THEORY AND METHODS

A. One-body Hamiltonian

Following the description in Ref. [34], a QD can be modeled as fermionic particles confined to two dimensions in a parabolic potential. The corresponding one-body Hamiltonian in such a potential is given in atomic units by

$$\hat{H}(x, y) = \frac{p_x^2 + p_y^2}{2} + \frac{1}{2}\omega^2(x^2 + y^2). \quad (1)$$

Here ω is a measure of the confinement strength of the electron in the parabolic potential well. Consequently, the Schrödinger equation can be separated into x and y coordinates, resulting in the differential equation for the 1D harmonic oscillator

$$\left(-\frac{1}{2}\frac{\partial^2}{\partial x^2} + \frac{\omega^2 x^2}{2}\right)\psi(x) = E\psi(x), \quad (2)$$

admitting the well-known solutions

$$\psi_n(x) = \frac{1}{\sqrt{2^n n!}} \left(\frac{\omega}{\pi}\right)^{1/4} e^{-\frac{\omega x^2}{2}} H_n(\sqrt{\omega}x),$$

$$E_n = \omega\left(n + \frac{1}{2}\right),$$

$$H_n(x) = (-1)^n e^{x^2} \frac{d^n}{dx^n} (e^{-x^2}),$$

where $n \in \mathbb{N}$. The corresponding solutions to the noninteracting 2D problem are

$$\psi_{nm}(x, y) = \psi_n(x)\psi_m(y), \quad (3)$$

$$E_{nm} = E_n + E_m = \omega(n + m + 1). \quad (4)$$

We note that the ground state is given by the solution with $m = 0$ and $n = 0$ and is nondegenerate. The first excited state is given by the solutions with $(n = 1, m = 0)$ and $(n = 0, m = 1)$ and has a degeneracy of 2. The second excited state is given by $(n = 2, m = 0)$, $(n = 0, m = 2)$, and $(n = 1, m = 1)$ and has a degeneracy of 3, and so forth.

B. Two-body Hamiltonian

The electronic structure of the 2D QD is strongly affected by electronic correlation effects caused by interelectronic interactions. To describe the true many-body nature of the 2D QD with N electrons, we have to include the two-body Coulomb interaction and consider the following two-body Hamiltonian:

$$\hat{H} = \sum_{i=1}^N \hat{H}(x_i, y_i) + \frac{1}{2} \sum_{i \neq j}^N \frac{1}{\sqrt{(x_i - x_j)^2 + (y_i - y_j)^2}}, \quad (5)$$

where $\hat{H}(x_i, y_i)$ is the one-body operator defined by Eq. (1). Herein we employ the bare Coulomb interaction. We note, however, that many model Hamiltonians for QDs account for screening effects by including various approximations to the permittivity in the interelectronic interaction. Given the fermionic character of the particles, the form and relative strength of the one-particle and two-particle operators of the above Hamiltonian, it is reasonable to assume that conventional quantum chemical many-electron wave function based methods yield reliable solutions for its ground and excited states. In this hierarchy of quantum chemical wave function based methods, the HF theory, employing a self-consistent field approximation, is a well-established starting point.

C. HF and post-HF theory

The HF method is one of the simplest wave function based *ab initio* approaches used in electronic structure theory calculations. It serves not only as a useful approximation in its own right but as the starting point of other more accurate models such as CC. In unrestricted HF (UHF) theory the many-body wave function is approximated by a single Slater determinant and the energy is optimized with respect to variations of the spin orbitals used to construct the Slater determinant. The Slater determinant formed from these spin orbitals is the UHF ground state wave function $|0\rangle$ and can be interpreted as a new vacuum from where particle-hole pairs are created and annihilated in the context of quantum field theory.

One way to improve the HF result is Møller-Plesset perturbation theory [93]. It adds electron-electron correlation effects by means of Rayleigh-Schödinger perturbation theory, usually to second order, commonly referred to as MP2.

Building on one-body theories such as UHF, coupled cluster theory employs an exponential ansatz acting on a single Slater determinant. Using $|0\rangle$ the ansatz reads

$$|\Psi_{CC}\rangle = e^{\hat{T}} |0\rangle, \quad (6)$$

$$\hat{T} = \sum_{i,a} t_i^a \hat{a}_a^\dagger \hat{a}_i + \frac{1}{4} \sum_{i,j,a,b} t_{ij}^{ab} \hat{a}_a^\dagger \hat{a}_b^\dagger \hat{a}_j \hat{a}_i + \dots, \quad (7)$$

where indices a, b, \dots and i, j, \dots denote virtual or particle and occupied or hole orbitals, respectively. \hat{a}^\dagger and \hat{a} are the second quantization creation and annihilation operators, creating excited Slater determinants when acting on the reference determinant. The cluster operator \hat{T} includes in principle all excitations up to the number of electrons in the system. Using this exponential form for the wave function ansatz in the stationary Schrödinger equation gives

$$\hat{H} |\Psi_{CC}\rangle = E_{CC} |\Psi_{CC}\rangle,$$

which is equivalent to

$$\bar{H} |0\rangle = E_{CC} |0\rangle, \quad (8)$$

where we have implicitly defined the similarity transformed Hamiltonian $\bar{H} = e^{-\hat{T}} \hat{H} e^{\hat{T}}$. In coupled cluster singles and doubles theory, the cluster operator \hat{T} is truncated such that it includes only singles and doubles excitations. In order to solve Eq. (8) for CCSD theory, one has to find the coefficients t_i^a and t_{ij}^{ab} . Working equations are commonly obtained by projecting the HF, singles and doubles manifold basis $\{|0\rangle, \hat{a}_a^\dagger \hat{a}_i |0\rangle, \hat{a}_a^\dagger \hat{a}_b^\dagger \hat{a}_j \hat{a}_i |0\rangle\}$ of the Slater determinant space onto Eq. (8):

$$E_{CC} = \langle 0 | \bar{H} | 0 \rangle, \quad (9)$$

$$0 = \langle 0 | \hat{a}_i^\dagger \hat{a}_a \bar{H} | 0 \rangle, \quad (10)$$

$$0 = \langle 0 | \hat{a}_i^\dagger \hat{a}_j^\dagger \hat{a}_b \hat{a}_a \bar{H} | 0 \rangle. \quad (11)$$

Equation (9) gives an expression for the CC energy and is valid also for nontruncated cluster operators \hat{T} . Equations (10) and (11) form a set of coupled nonlinear equations and can be solved for t_i^a and t_{ij}^{ab} using iterative methods [77,94].

It is worth noting that in the case of 2 electrons CCSD theory is exact and equivalent to FCI.

A successful method of obtaining excited states from CC theory is to diagonalize the Hamiltonian \bar{H} in a suitable subspace of the Hilbert space. This is the main approach followed in the equation of motion coupled cluster (EOM-CC) method. In this work we use the charge-neutral variant of this methodology, the electron excitation EOM-CC (EE-EOM-CC) theory [86,87]. The theory is based on a linear ansatz for the excitation operators \hat{R} as in FCI, thus the main working equations read

$$\hat{H} \hat{R} |\Psi_{CC}\rangle = E_R \hat{R} |\Psi_{CC}\rangle, \quad (12)$$

$$\hat{R} = r_0 + \sum_{i,a} r_i^a \hat{a}_a^\dagger \hat{a}_i + \frac{1}{4} \sum_{i,j,a,b} r_{ij}^{ab} \hat{a}_a^\dagger \hat{a}_b^\dagger \hat{a}_j \hat{a}_i + \dots \quad (13)$$

The scalars $\{r_0, r_i^a, r_{ij}^{ab}, \dots\}$ define the excitation operator \hat{R} and are to be determined, whereas E_R is its excitation energy.

Equation (12) is equivalent to a commutator equation only involving \bar{H} and the excitation energy difference ΔE_R between E_R and E_{CC} :

$$[\bar{H}, \hat{R}] |0\rangle = (E_R - E_{CC}) \hat{R} |0\rangle. \quad (14)$$

Note that in the commutator on the left-hand side only connected diagrams need to be considered in the CI expansion. In this work we use the spin-flip version of EOM-CC [87,95], whereby no spin-conserving restrictions are imposed to the $r_i^a, r_{ij}^{ab}, \dots$ amplitudes. Moreover, all excited state calculations are performed employing the EE-EOM-CCSD approach, where only up to two-body excitation operators are considered. Analogously to CCSD, EE-EOM-CCSD is exact for 2 electrons.

D. Matrix elements

In order to apply CCSD theory to find approximate solutions for the ground state of the 2D QD model Hamiltonian represented in a given orbital basis, one has to compute the Coulomb integrals

$$\int_{-\infty}^{\infty} \int_{-\infty}^{\infty} \int_{-\infty}^{\infty} \int_{-\infty}^{\infty} dx_1 dx_2 dy_1 dy_2 \times \frac{\psi_{nm}^*(x_1, y_1) \psi_{op}^*(x_2, y_2) \psi_{qr}(x_1, y_1) \psi_{st}(x_2, y_2)}{\sqrt{(x_1 - x_2)^2 + (y_1 - y_2)^2}}, \quad (15)$$

where ψ_{nm} are the two-dimensional orbitals introduced in Eq. (3). For Gaussian based basis sets and their derivatives, methods for analytical computation of such integrals exist, which are commonly based on recursive relations and can be implemented on a computer using code generation facilities [96–98].

In this work we present a numerical approach for Coulomb integrals evaluation that is computationally less efficient but can be applied to arbitrary orbitals. This can potentially be useful for model Hamiltonians represented in a set of basis functions that are difficult to expand using Gaussian functions or their derivatives but can be well represented on a sufficiently dense spatial grid.

The main idea of our approach is to assume that the singular Coulomb kernel exhibits a more rapid spatial variation than the orbitals and that the employed real space grid is dense enough to approximate the orbitals by a constant inside any volume/area sampled by the grid. Based on this premise, we discretize the wave function and integrate over discretized hypercubic volume elements with an edge length of Δx . The way in which this was done is described in detail in Appendix A. The resulting numerical expression for the Coulomb integral (15) can be rewritten as a sum:

$$\sum_{ijkl} \psi_{nm}^*(x_i, y_j) \psi_{op}^*(x_k, y_l) \psi_{qr}(x_i, y_j) \psi_{st}(x_k, y_l) a_{i-k, j-l} \Delta x^3, \quad (16)$$

where a_{ij} is a system independent matrix that does not depend on Δx . $\{i, j, k, l\}$ are here discretization indices and are not to be confused with hole indices. Note that the factor Δx^3 implies that a_{ij} is dimensionless. Additionally, we reiterate that

TABLE I. Summary of the convergence of CCSD energies for the $N = 2$ electron system with $\omega = 1.0$ as a function of the number of grid points N_g used to represent the wave function. The CCSD energies have been computed for a finite basis set corresponding to 6 oscillator shells or 21 orbitals. All energies are in Hartree.

Δx (a.u.)	N_g	CCSD
0.1025	100×100	3.013673
0.0513	200×200	3.013621
0.0342	300×300	3.013613
0.0256	400×400	3.013610
0.0205	500×500	3.013612
0.0171	600×600	3.013613

although this approach is computationally significantly less efficient than the recursive scheme, the computational bottleneck in the present study remains in the EE-EOM-CCSD calculations.

III. RESULTS

We study QDs for a range of electron numbers and $\omega \in \{1.0, 0.5, 0.28\}$. ω characterizes the correlation strength in the system relative to the potential energy. Large ω correspond to weakly correlated systems, whereas small ω correspond to stronger correlated systems [75].

Throughout this section all quantities are presented in atomic units (a.u.). In particular, all energy values are therefore given in Hartree.

A. Ground state energies

We first discuss the numerical reliability of our approach. Let us note that our approach employs a single computational parameter Δx , which defines the grid spacing used for the real space representation of all orbitals and the numerical integration. Table I shows the computed CCSD energies of the two electron system with $\omega = 1.0$ for a range of Δx . Our findings show that 300×300 grid points suffice to achieve sub-mHa precision. For all further Coulomb integral calculations, we have therefore discretized the wave function into squares of edge length $\Delta x = 0.0342$ a.u., in a range where $|\psi(x, y)|^2 > 10^{-10}$. However, we note that a careful comparison between results summarized in our work and Refs. [75,90] reveals that the published CCSD ground state energies do not always agree to within mHa. We attribute these discrepancies to different choices of basis sets in the CCSD and Hartree-Fock calculations, which can result in a different convergence behavior of the energies to the complete basis set limit. Our basis set extrapolation approach will be discussed in the following paragraphs.

Having assessed the reliability of our numerical approach, we now turn to the discussion of the ground state results obtained on the level of HF, MP2, and CCSD theories. We stress that it is necessary to converge all post-HF correlation energies with respect to the employed orbital basis set. For three-dimensional *ab initio* systems and the uniform electron gas [99], it is known from second-order perturbation theory that the basis set error scales as $1/N_v$, where N_v refers to

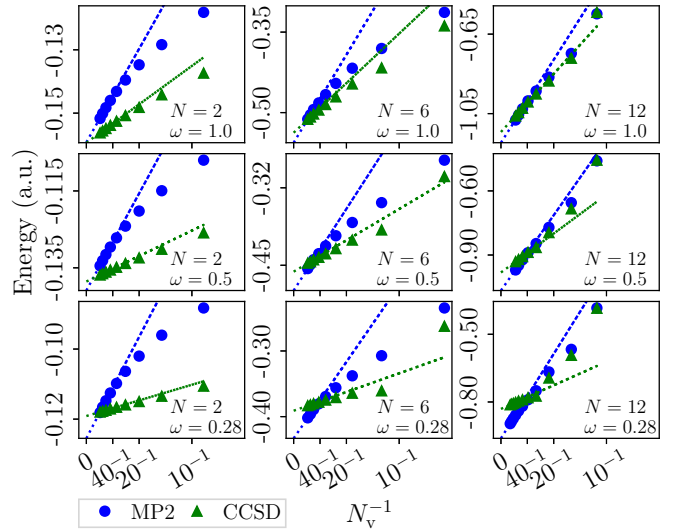


FIG. 1. CCSD and MP2 correlation energies and their CBS extrapolations for $N \in \{2, 6, 12\}$ electron systems with $\omega \in \{1.0, 0.5, 0.28\}$ as a function of the inverse number of virtual orbitals. All energies are presented in Hartree and ω is given in atomic units.

the number of virtual orbitals. The complete basis set limit is obtained by extrapolating $N_v \rightarrow \infty$.

For the studied system, the two-dimensional QD, we expect a similar behavior for the correlation energies. In order to motivate the validity of this assumption, we have shown analytically that the asymptotic relation holds for the second-order perturbation theory correlation energy. Details regarding the derivation can be found in Appendix B.

Numerical results for the correlation energies retrieved as a function of $1/N_v$ are depicted in Fig. 1 and confirm this behavior for both MP2 and CCSD. From these numerical findings we conclude that the correlation energies can be linearly fitted using the following formula: $E(N_v) = E_{\text{CBS}} + \frac{A}{N_v}$ with parameters (E_{CBS}, A) .

Throughout this work E_{CBS} refers to extrapolated complete basis set limit energies that have been obtained by fitting the latter function using energies obtained with 65 and 77 orbitals.

It is worth noting that in the specific case of $\omega = 1.0$ for the 2 electron quantum dot the exact energy $E = 3.0$ is available from the literature [75,100] also a variationally achieved energy as a function of ω that agrees to 5 decimal places with the analytic solution is available [91]. Comparing our CBS energy with the analytic solution $E = 3.0$ leaves a discrepancy that we attribute to the extrapolation scheme. The $1/N_v$ extrapolation captures the leading order finite basis set errors. However, as evident from the convergence in Table II, other terms also contribute to the basis set error and sufficiently large N_v have to be used in order for the $1/N_v$ extrapolation to obtain reliable results. Our analysis shows that including higher order terms in the extrapolation scheme brings us even closer to the exact energy. However, technically it is simpler and more robust to use only the leading term. Furthermore, increasing the basis set size also brings us closer to the exact CBS limit, summarized in Table III. But at this point we cannot afford larger basis set sizes.

TABLE II. Summary of CBS limit CCSD ground state energy for the 2 electron system with $\omega = 1.0$, with different functions used for the extrapolation. All energies are in Hartree.

Extrapolation function	E_{CBS}
$E_{\text{CBS}} + \frac{a}{N_v}$	3.00217
$E_{\text{CBS}} + \frac{a}{N_v} + \frac{b}{N_v^{\frac{2}{3}}}$	3.00147
$E_{\text{CBS}} + \frac{a}{N_v} + \frac{b}{N_v^{\frac{2}{3}}} + \frac{c}{N_v^2}$	3.00083

Table IV summarizes the HF, MP2, and CCSD correlation energies together with the CBS limit for $\omega \in \{1.0, 0.5, 0.28\}$ for the 2 electron system. Compared to the HF energy, the MP2 correlation energy changes only slightly with ω . However, on a relative scale the importance of the correlation energy contribution to the ground state energy increases from 5.3% to 11.7% (ratio of MP2/CCSD correlation energy and the ground state energy for $N = 2$, $\omega = 1.0$ and 0.28 a.u.). Low-order perturbation theories like MP2 become less reliable in the regime of strong correlation. CCSD, being a more accurate theory in the sense that it contains all contributions from MP3 theory and beyond, is expected to yield more accurate results than MP2 for small ω . We can see that the relative CCSD and MP2 contributions to the ground state energy differ more as ω decreases.

The linear scaling of the correlation energies with ω and the basis set convergence shown in Fig. 1 is found to be qualitatively independent of the number of electrons. All calculated CBS ground state energies are summarized in Table V for further reference. Our findings demonstrate that small electron numbers already serve as a good approximation to the behavior of ground state energies with the investigated parameters.

B. Excitation energies

Having established a procedure to converge the ground state energies with the basis set, we now seek to discuss the excited state properties. To this end we employ EE-EOM-CCSD theory and the same Hamiltonian employed in the previous section. We have calculated the first three excitation energies, where the first excited state in EE-EOM-CCSD theory corresponds to a triplet state while the second and third excited states are singlet states.

Analogously to the ground state, we need to converge the excitation energies carefully with the basis set. Figures 2–4 give evidence that the EE-EOM-CCSD excitation energies converge in a similar manner to the complete basis set limit. However, the slope is significantly less steep, resulting in exci-

TABLE III. Summary of CBS limit CCSD ground state energy for the 2 electron system with $\omega = 1.0$, with different basis set sizes used for the extrapolation. All energies are in Hartree.

N_v	E_{CBS}
44–54	3.00259
54–65	3.00238
65–77	3.00217

TABLE IV. HF energy and correlation energy contributions on the level of MP2 and CCSD theory in Hartree for 2 electrons. N_v denotes the number of virtual orbitals, with its value at ∞ being the extrapolated value. Our results show that as ω increases, the HF ground state energies increases linearly with ω . HF is a good approximation in the limit of large ω where the interelectronic interaction is small compared to the one-body interaction.

ω (a.u.)	N_v	HF	MP2	CCSD
1.0	9	3.1626	−0.1182	−0.1374
	14	3.1618	−0.1284	−0.1442
	20	3.1618	−0.1347	−0.1482
	27	3.1618	−0.1395	−0.1508
	35	3.1618	−0.1431	−0.1526
	44	3.1618	−0.146	−0.1539
	54	3.1618	−0.1483	−0.1548
	65	3.1618	−0.1501	−0.1556
	77	3.1618	−0.1517	−0.1562
	∞	3.1618	−0.1602	−0.1596
0.5	9	1.7998	−0.107	−0.1259
	14	1.7997	−0.1149	−0.1302
	20	1.7997	−0.1202	−0.1324
	27	1.7997	−0.1242	−0.1339
	35	1.7997	−0.1272	−0.1348
	44	1.7997	−0.1296	−0.1356
	54	1.7997	−0.1315	−0.1361
	65	1.7997	−0.1331	−0.1365
	77	1.7997	−0.1345	−0.1369
	∞	1.7997	−0.1418	−0.1387
0.28	9	1.1417	−0.0962	−0.1129
	14	1.1417	−0.102	−0.1151
	20	1.1417	−0.1065	−0.1162
	27	1.1417	−0.1098	−0.1169
	35	1.1417	−0.1123	−0.1174
	44	1.1417	−0.1144	−0.1178
	54	1.1417	−0.1161	−0.1181
	65	1.1417	−0.1174	−0.1183
	77	1.1417	−0.1186	−0.1185
	∞	1.1417	−0.1249	−0.1194

tation energies with relatively small basis set incompleteness errors when employing $N_v = 77$. Note that in the case of $N = 12$ and $\omega = 0.28$ we use $N_v = 114$ for the extrapolation.

TABLE V. Summary of CBS limit CCSD energies for $N \in \{2, 6, 12\}$ electron systems with $\omega \in \{1.0, 0.5, 0.28\}$. All energies are in Hartree.

ω (a.u.)	Electrons	E_{CBS}
1.0	2	3.0022
	6	20.1839
	12	65.7644
0.5	2	1.6609
	6	11.8118
	12	39.2343
0.28	2	1.0222
	6	7.6292
	12	25.7190

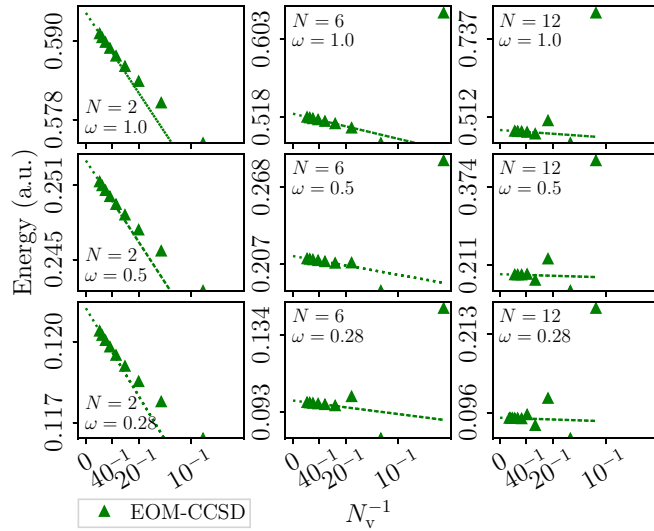


FIG. 2. First EE-EOM-CCSD excitation energy for $N \in \{2, 6, 12\}$ electron systems with $\omega \in \{1.0, 0.5, 0.28\}$ retrieved as a function of the inverse number of virtual orbitals N_v^{-1} . All energies are in Hartree.

We estimate the CBS limit of the excitation energies using an identical extrapolation procedure as outlined in the previous section. In the case of excited states, as seen in Figs. 2–4, the slope of the extrapolation function is less steep, resulting in a more reliable result.

Figure 5 shows the first excitation energy (singlet-triplet gap) for $N = 2$ as a function of ω . EE-EOM-CCSD calculations predict an excitation energy that decreases with decreasing ω . Approximating the singlet-triplet gap on the level of UHF theory yields an intersystem crossing at $\omega = 0.3926$ a.u. However, UHF energies neglect correlation effects, which are expected to be larger in magnitude for the

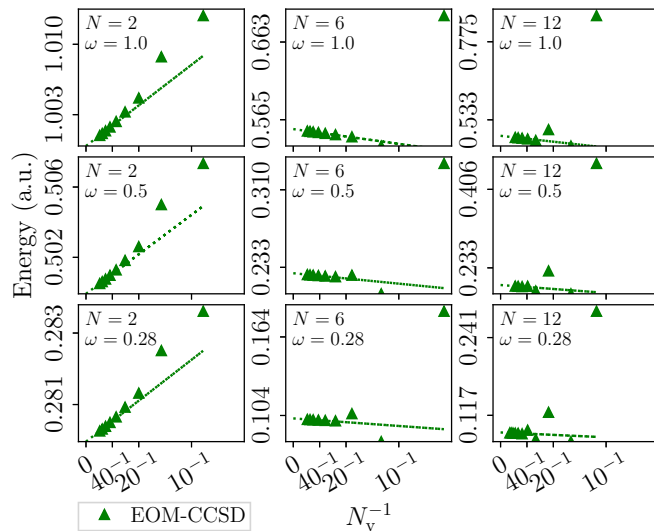


FIG. 3. Second EE-EOM-CCSD excitation energy for $N \in \{2, 6, 12\}$ electron systems with $\omega \in \{1.0, 0.5, 0.28\}$ retrieved as a function of the inverse number of virtual orbitals N_v^{-1} . All energies are in Hartree.

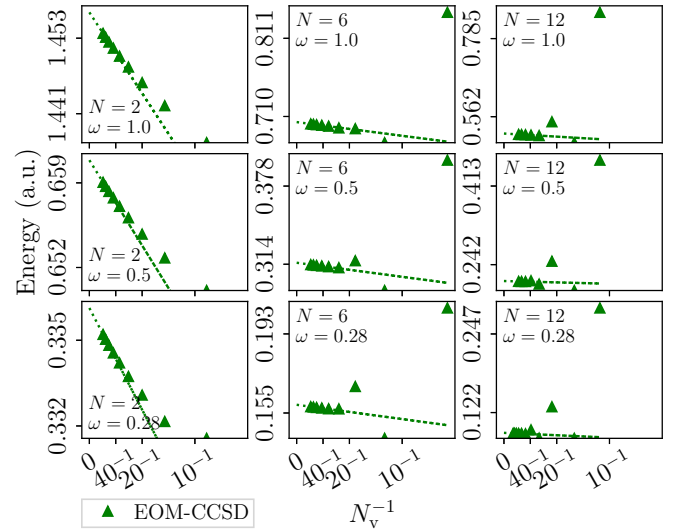


FIG. 4. Third EE-EOM-CCSD excitation energy for $N \in \{2, 6, 12\}$ electron systems with $\omega \in \{1.0, 0.5, 0.28\}$ retrieved as a function of the inverse number of virtual orbitals N_v^{-1} . All energies are in Hartree.

singlet state than for the triplet state. It has already been discussed that the singlet-triplet crossing predicted by UHF results from the neglect of the electron-electron correlation [45]. Indeed, we find that UMP2 and EOM-CC theory predict no singlet-triplet crossing. Details on how the UMP2 and UHF singlet-triplet gap was calculated can be found in Appendix C.

Finally, Table VI summarizes the CBS excitation energies from Figs. 2–4. It shows that the linear scaling of the excitation energies with ω is qualitatively unchanged when comparing $N = 2$, $N = 6$, and $N = 12$ electron systems.

Our findings show that all excitation energies scale linearly with ω .

For the 2 electron quantum dot the singlet-singlet excitations (in our work the second and third excitation) are

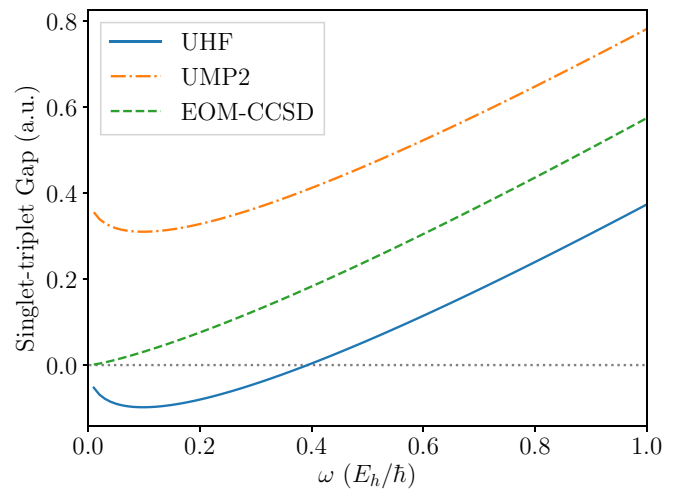


FIG. 5. Singlet-triplet gap calculated with UHF, UMP2, and EE-EOM-CCSD as a function of ω in Hartree. All calculations are done with $N_v = 10$.

TABLE VI. CBS limit excitation energies for $N \in \{2, 6, 12\}$ electron systems with $\omega \in \{1.0, 0.5, 0.28\}$. All quantities are expressed in atomic units.

ω (a.u.)	Electrons	First excitation	Second excitation	Third excitation
1.0	2	0.5943	0.9999	1.4571
	6	0.5218	0.5532	0.7028
	12	0.4752	0.4834	0.5138
0.5	2	0.2530	0.4999	0.6609
	6	0.2136	0.2271	0.3152
	12	0.1913	0.1951	0.2063
0.28	2	0.1212	0.2800	0.3361
	6	0.0991	0.1018	0.1589
	12	0.0883	0.0897	0.0897

variationally available [91]. We have compared our singlet-singlet excitation energies to values from Ref. [91] and they are in excellent agreement as summarized in Table VII. The remaining differences of the excitation energies can be attributed to the CBS extrapolation procedure and also to the numerical procedures regarding the Coulomb integrals and the wave function, as described in the previous section.

IV. CONCLUSION AND SUMMARY

In this paper we have investigated a model Hamiltonian for two-dimensional QDs using quantum chemical many-electron theories including HF, MP2, and CCSD. For the study of excited states we have employed the equation-of-motion formalism of CCSD theory (EOM-CCSD). We have outlined a numerical method to compute the Coulomb integrals for arbitrary orbitals represented on a discrete numerical grid. Although this method is computationally less efficient than recursive schemes for orbitals that correspond to Gaussians or their derivatives, we note that it can become potentially useful for different model Hamiltonians that include a one-body part and corresponding eigenfunctions which are difficult to expand using Gaussians or their derivatives.

We have investigated the convergence of the computed correlation energies for ground and excited states with respect to the number of virtual orbitals numerically, finding a convergence behavior for two-dimensional QDs which is identical to the basis set convergence of the second-order correlation energy in perturbation theory of the three-dimensional electron gas. Furthermore, we have performed an analytic derivation for the two-dimensional QD on the level of second-order perturbation theory that supports this convergence behavior.

TABLE VII. CBS limit ground state and excitation energies for the 2 electron system with $\omega \in \{1.0, 0.5\}$ compared to the variationally optimized energies from Ref. [91] on the right. All quantities are expressed in atomic units.

ω (a.u.)	Ground state	Second excitation	Third excitation
1.0	3.002/3.000	1.000/1.000	1.457/1.459
0.5	1.661/1.660	0.500/0.500	0.661/0.662

Based on this analysis, we have extrapolated all computed correlation energies for ground and excited states to the complete basis set limit assuming a $1/N_v$ convergence of the remaining finite basis set errors and compared them partly to analytic and variationally achieved semianalytic results.

The computed ground state energies in a range of $\omega = 0.28$ a.u., which corresponds to a strongly correlated regime, to $\omega = 1.0$ a.u., has revealed that the HF energy scales linearly with respect to ω and that the relative contribution of the MP2 and CCSD correlation energies to the ground state energy increases with decreasing ω . Furthermore, we have observed that with decreasing ω the relative difference between the MP2 and CCSD correlation energy is increasing, outlining that CCSD captures higher order correlation effects than MP2.

Using the EE-EOM-CCSD formalism, we have calculated the first three excitation energies of the QD and partly compared them to values from the literature. Our findings show that the excitation energies scale linearly with ω and for $N = 12$ and $\omega = 0.28$ the second and third excitation become numerically degenerate.

Finally, our work also demonstrates that two-dimensional QD model Hamiltonians serves not only as a suitable tool for experimental QDs but can also be used as efficient and well-controlled testing ground of approximate many-electron theories to study ground and excited state properties. Using a single parameter to tune the confinement via the harmonic potential, the Hamiltonian can be modified to switch between different regimes of correlation strengths and investigate the accuracy of finite-order perturbation theories. However, we find that EOM-CCSD performs qualitatively correctly for the investigated parameter ranges and that the remaining errors are expected to be only of quantitative interest. In future work we seek to investigate different levels of EOM theories and compare to other widely used electronic structure theories that treat ground and excited state phenomena.

ACKNOWLEDGMENTS

The authors thankfully acknowledge support and funding from the European Research Council (ERC) under the European Unions Horizon 2020 research and innovation program (Grant Agreement No. 715594). The computational results presented have been achieved in part using the Vienna Scientific Cluster (VSC).

APPENDIX A: ANALYTIC SOLUTION OF THE INTEGRAL OVER THE 2D COULOMB KERNEL

To perform the integration in Eq. (15) we discretize the integration domain into hypercubes with an edge length of Δx centered at x_i, x_j, y_k, y_l :

$$\sum_{ijkl} \int_{x_i - \frac{\Delta x}{2}}^{x_i + \frac{\Delta x}{2}} \int_{x_j - \frac{\Delta x}{2}}^{x_j + \frac{\Delta x}{2}} \int_{y_k - \frac{\Delta x}{2}}^{y_k + \frac{\Delta x}{2}} \int_{y_l - \frac{\Delta x}{2}}^{y_l + \frac{\Delta x}{2}} \psi_{mnopqrst}(x_1, y_1, x_2, y_2) \frac{dx_1 dx_2 dy_1 dy_2}{\sqrt{(x_1 - x_2)^2 + (y_1 - y_2)^2}} \quad (\text{A1})$$

With $i, j, k, l \in \mathbb{Z}$, $x_i = i\Delta x$, $x_j = j\Delta x$, $y_k = k\Delta x$, $y_l = l\Delta x$, and

$$\psi_{mnopqrst} = \psi_{mn}^* \psi_{op}^* \psi_{qr} \psi_{st}. \quad (\text{A2})$$

Employing simple quadrature, we approximate the wave function from (A1) to be constant within each integration block:

$$\sum_{ijkl} \psi_{mnopqrst}(x_i, y_j, x_k, y_l) \iiint \frac{dx_1 dx_2 dy_1 dy_2}{\sqrt{(x_1 - x_2)^2 + (y_1 - y_2)^2}}. \quad (\text{A3})$$

This leaves us with the integral over the Coulomb kernel, which cannot be treated in the same manner due to points with $x_i = x_j$ and $y_k = y_l$, where the Coulomb kernel becomes sin-

gular. We solve this problem using the Laplace transformation of the Coulomb kernel, leading to a simplified expression. We start with

$$\int_{x_i - \frac{\Delta x}{2}}^{x_j + \frac{\Delta x}{2}} \int_{x_j - \frac{\Delta x}{2}}^{x_j + \frac{\Delta x}{2}} \int_{y_k - \frac{\Delta x}{2}}^{y_l + \frac{\Delta x}{2}} \int_{y_l - \frac{\Delta x}{2}}^{y_l + \frac{\Delta x}{2}} \frac{dx_1 dx_2 dy_1 dy_2}{\sqrt{(x_1 - x_2)^2 + (y_1 - y_2)^2}}. \quad (\text{A4})$$

Applying the Laplace transformation

$$\frac{1}{|\vec{r}_1 - \vec{r}_2|} = \frac{2}{\sqrt{\pi}} \int_0^\infty dt e^{-t^2(|\vec{r}_1 - \vec{r}_2|)^2} \quad (\text{A5})$$

yields

$$\frac{2}{\sqrt{\pi}} \int_0^\infty dt \int_{-\frac{\Delta x}{2}}^{\frac{\Delta x}{2}} \int_{\Delta i \Delta x - \frac{\Delta x}{2}}^{\Delta i \Delta x + \frac{\Delta x}{2}} dx_1 dx_2 e^{-t^2(x_1 - x_2)^2} \int_{-\frac{\Delta x}{2}}^{\frac{\Delta x}{2}} \int_{\Delta j \Delta x - \frac{\Delta x}{2}}^{\Delta j \Delta x + \frac{\Delta x}{2}} dy_1 dy_2 e^{-t^2(y_1 - y_2)^2}, \quad (\text{A6})$$

with $\Delta i = i - k$ and $\Delta j = j - l$. The integration over x_1 and x_2 :

$$\int_{-\frac{\Delta x}{2}}^{\frac{\Delta x}{2}} \int_{\Delta i \Delta x - \frac{\Delta x}{2}}^{\Delta i \Delta x + \frac{\Delta x}{2}} dx_1 dx_2 e^{-t^2(x_1 - x_2)^2} \quad (\text{A7})$$

can be done analytically using the error function, analogously for y_1 and y_2 . The result is

$$F(\Delta i, t) = \frac{1}{2t^2} (e^{-\Delta x^2(\Delta i - 1)^2 t^2} - 2e^{-\Delta x^2 \Delta i^2 t^2} + e^{-\Delta x^2(\Delta i + 1)^2 t^2} + \Delta x \sqrt{\pi} t \{-2\Delta i \text{erf}(\Delta x \Delta i t) + (\Delta i + 1) \text{erf}[\Delta x(\Delta i + 1)t] - (\Delta i - 1) \text{erf}[\Delta x(-\Delta i + 1)t]\}).$$

And this leaves us with a 1D integral over the variable t for every Δi and Δj ,

$$a(\Delta i, \Delta j) = \frac{2}{\sqrt{\pi}} \int_0^\infty dt F(\Delta i, t) F(\Delta j, t). \quad (\text{A8})$$

As it can be seen in Fig. 6 the integrand $F(\Delta i, t)F(\Delta j, t)$ is well behaved and can be integrated numerically without much computational cost. In some special cases, for example $\Delta i = \Delta j = 0$, the analytic solution is available:

$$\int_{-\frac{\Delta x}{2}}^{\frac{\Delta x}{2}} \int_{-\frac{\Delta x}{2}}^{\frac{\Delta x}{2}} \int_{-\frac{\Delta x}{2}}^{\frac{\Delta x}{2}} \int_{-\frac{\Delta x}{2}}^{\frac{\Delta x}{2}} \frac{dx_1 dx_2 dy_1 dy_2}{\sqrt{(x_1 - x_2)^2 + (y_1 - y_2)^2}} = -\frac{4}{3}(\sqrt{2} - 1 - 3 \text{asinh}(1)) \Delta x^3. \quad (\text{A9})$$

But for the general case $\Delta i \neq \Delta j$ we have to solve the integral numerically.

The functional form of the integral is not dependent on the domain of integration. Therefore the integral will always be proportional to Δx^3 times a constant $a(\Delta i, \Delta j)$. Note that the constants $a(\Delta i, \Delta j)$ are not dependent on Δx . Equation (A1) can be rewritten as

$$\sum_{ijkl} \psi_{mnopqrst}(x_i, y_j, x_k, y_l) a(\Delta i, \Delta j) \Delta x^3. \quad (\text{A10})$$

We now evaluate the Coulomb integrals in real space numerically. Note that the constants $a(\Delta i, \Delta j)$ only need to be computed once and can be used for every Δx . Δi and Δj define the distance of the integration region from the singularity in steps of Δx . Approximating the Coulomb kernel by a constant in the region of integration becomes more accurate with increasing distance from the singularity. So a cutoff has to be chosen where the distance to the singularity is big enough such that we can use the constant approximation. With $\Delta i = 25$ and $\Delta j = 0$ Eq. (A4) with the constant approxima-

tion gives $0.04\Delta x^3$, while evaluated with our scheme it gives $0.0400054\Delta x^3$. Thus we have chosen $\Delta i = 25$ as cutoff.

Note that this evaluation scheme for the Coulomb integrals can be generalized to three-dimensional systems straightforwardly.

APPENDIX B: ASYMPTOTIC BEHAVIOR OF THE CORRELATION ENERGY

In order to extrapolate to the complete basis set limit of the correlation energy, we need to derive an expression that yields that basis set truncation error as a function of the number of virtual orbitals. The correlation energy in second-order perturbation theory is given by

$$E_{\text{corr}} = \sum_k \frac{|\langle 0 | g_{ij} | k \rangle|^2}{E_k - E_0}. \quad (\text{B1})$$

Where $|0\rangle$ denotes the ground state, k is a excited state of the unperturbed Hamiltonian, and E_0 and E_k are the corresponding energies. In theory, the summation goes over all excited states but in practice we have to truncate the summation at

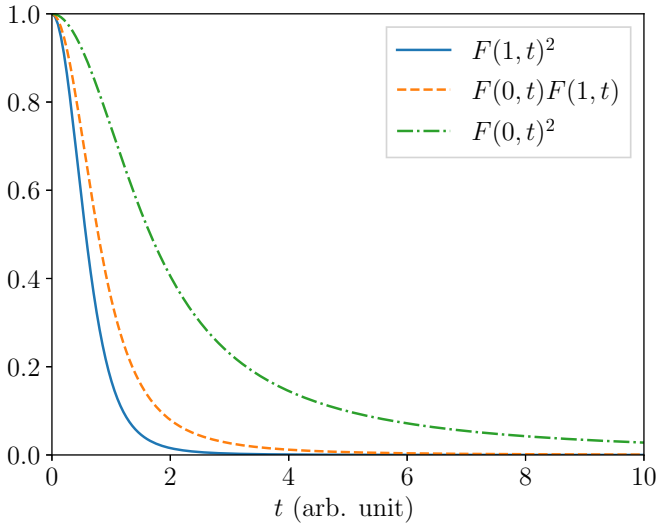


FIG. 6. $F(1, t)^2$, $F(0, t)F(1, t)$, $F(0, t)^2$ from left to right. See main text for more details.

some cutoff k_{cut} . To replace the cutoff energy with the number of virtual orbitals in the above equation, we have to employ Eqs. (3) and (4). We are only interested in the asymptotic behavior of the cutoff error, which is defined by

$$E_{\text{err}} = \lim_{N_v \rightarrow \infty} \sum_{k_{\text{cut}}}^{\infty} \frac{|\langle 0 | \frac{1}{r_{ij}} | k \rangle|^2}{E_k - E_0}. \quad (\text{B2})$$

Furthermore, we can use the formula

$$\lim_{n \rightarrow \infty} e^{-\frac{x^2}{2}} H_n(x) \sim \frac{2^n}{\sqrt{\pi}} \Gamma\left(\frac{n+1}{2}\right) \cos\left(x\sqrt{2n} - \frac{n\pi}{2}\right) \quad (\text{B3})$$

to approximate our excited states with a simple cos function. Now the Coulomb integral can be calculated analytically, which leaves us with the result

$$\lim_{R \rightarrow \infty} \langle (00), (00) | \frac{1}{r_{ij}} | (RR), (RR) \rangle = \frac{4^R \Gamma\left(\frac{1+R}{2}\right)^4}{\pi^4 (R!)^2}, \quad (\text{B4})$$

where R denotes the shell of the orbital. Inserting this result into Eq. (B2) and using the approximation for the gamma function

$$\lim_{x \rightarrow \infty} \Gamma(x+1) \sim \sqrt{2\pi x} \left(\frac{x}{e}\right)^x \quad (\text{B5})$$

gives us

$$E_{\text{err}} = \sum_R \frac{4(R-1)^2}{\pi^6 R^5}. \quad (\text{B6})$$

In the above equation, the sum can be replaced by an integration, yielding

$$E_{\text{err}} = \frac{4}{\pi^6} \left(-\frac{1}{2R^2} + \frac{2}{3R^3} - \frac{1}{4R^4} \right). \quad (\text{B7})$$

As the final step we have to convert the shell R to the number of orbitals N_v . By assuming filled shells we can write

$$R = \frac{1 + \sqrt{8N_v + 1}}{2}, \quad (\text{B8})$$

which gives us the final result for the basis set error of second-order perturbation theory correlation energies computed using a truncated basis in the limit of $N_v \rightarrow \infty$:

$$\lim_{N_v \rightarrow \infty} E_{\text{err}} \sim \frac{1}{N_v}. \quad (\text{B9})$$

APPENDIX C: SINGLET TRIPLET GAP CALCULATION

In order to calculate the singlet and triplet ground state energy of the 2 electron QD with HF and MP2 theory the following Slater determinants have been used:

$$|\Psi_{\text{singlet}}\rangle = |(00, \uparrow)(00, \downarrow)\rangle,$$

$$|\Psi_{\text{triplet}}\rangle = |(00, \uparrow)(01, \uparrow)\rangle.$$

The HF ground state energy for the 2 electron QD is given by

$$E_{\text{HF}} = \langle \Psi_{\text{gs}} | \hat{H} | \Psi_{\text{gs}} \rangle + \langle \Psi_{\text{gs}} | \hat{V} | \Psi_{\text{gs}} \rangle,$$

where \hat{H} is the single-body part of the Hamiltonian and \hat{V} is the Coulomb repulsion between the electrons. Inserting the ansatz for the wave functions of singlet and triplet states and applying the Slater-Condon rules gives

$$E_s = \omega + \langle 0000 | 0000 \rangle,$$

$$E_t = 2\omega + \langle 0001 | 0001 \rangle - \langle 0000 | 0101 \rangle.$$

The MP2 ground state energy is

$$E_{\text{MP2}} = E^{(0)} + E^{(1)} + E^{(2)},$$

$$E^{(0)} = \langle \Psi_{\text{gs}} | \hat{H} | \Psi_{\text{gs}} \rangle,$$

$$E^{(1)} = \langle \Psi_{\text{gs}} | \hat{V} | \Psi_{\text{gs}} \rangle,$$

$$E^{(2)} = \sum_{k \neq \Psi_{\text{gs}}} \frac{|\langle k | \hat{V} | \Psi_{\text{gs}} \rangle|^2}{E_k - E_{\text{gs}}}.$$

Applying the Slater-Condon rules and using the same singlet and triplet wave functions as for HF yields a additional contribution to the HF energy

$$E_{\text{MP2,s}} = E_s + \sum_{abcd} \frac{|\langle 0000 | abcd \rangle - \langle 00ab | 00cd \rangle|^2}{\omega(-a-b-c-d)},$$

$$E_{\text{MP2,t}} = E_t + \sum_{abcd} \frac{|\langle 0001 | abcd \rangle - \langle 00ab | 01cd \rangle|^2}{\omega(1-a-b-c-d)}.$$

[1] D. Bimberg and U. W. Pohl, *Mater. Today* **14**, 388 (2011).

[2] C.-Y. Han, H.-S. Kim, and H. Yang, *Materials* **13**, 897 (2020).

[3] S. Kargozar, S. J. Hoseini, P. B. Milan, S. Hooshmand, H.-W. Kim, and M. Mozafari, *Biotechnology J.* **15**, 2000117 (2020).

- [4] Y. Sajeev and N. Moiseyev, *Phys. Rev. B* **78**, 075316 (2008).
- [5] N. Ganguli, S. Acharya, and I. Dasgupta, *Phys. Rev. B* **89**, 245423 (2014).
- [6] G. Bester, S. Nair, and A. Zunger, *Phys. Rev. B* **67**, 161306(R) (2003).
- [7] R. Singh and G. Bester, *Phys. Rev. Lett.* **103**, 063601 (2009).
- [8] P. Walter, E. Welcomme, P. Hallégot, N. J. Zaluzec, C. Deeb, J. Castaing, P. Veyssière, R. Bréniaux, J.-L. Lévêque, and G. Tsoucaris, *Nano Lett.* **6**, 2215 (2006).
- [9] R. C. Ashoori, *Nature* **379**, 413 (1996).
- [10] A. Henglein, *Chem. Rev.* **89**, 1861 (1989).
- [11] M. Sundaram, S. A. Chalmers, P. F. Hopkins, and A. C. Gossard, *Science* **254**, 1326 (1991).
- [12] R. Cingolani and K. Ploog, *Adv. Phys.* **40**, 535 (1991).
- [13] A. P. Alivisatos, *Science* **271**, 933 (1996).
- [14] N. F. Johnson, *J. Phys.: Condens. Matter* **7**, 965 (1995).
- [15] C. Sloggett and O. P. Sushkov, *Surf. Sci.* **601**, 5788 (2007), Wagga Symposium on Surfaces and Interfaces - 2006.
- [16] S. Akbar and I.-H. Lee, *Phys. Rev. B* **63**, 165301 (2001).
- [17] F. Bolton, *Phys. Rev. Lett.* **73**, 158 (1994).
- [18] P. A. Maksym and T. Chakraborty, *Phys. Rev. Lett.* **65**, 108 (1990).
- [19] B. Partoens, A. Matulis, and F. M. Peeters, *Phys. Rev. B* **59**, 1617 (1999).
- [20] F. Holka, P. Neogrady, V. Kellö, M. Urban, and G. H. F. Dierksen, *Mol. Phys.* **103**, 2747 (2005).
- [21] N. M. Parzuchowski, T. D. Morris, and S. K. Bogner, *Phys. Rev. C* **95**, 044304 (2017).
- [22] L. P. Kouwenhoven, T. H. Oosterkamp, M. W. S. Danoesastro, M. Eto, D. G. Austing, T. Honda, and S. Tarucha, *Science* **278**, 1788 (1997).
- [23] H. Yakobi, E. Eliav, and U. Kaldor, *J. Chem. Phys.* **134**, 054503 (2011).
- [24] C. Metzner and G. H. Döhler, *Phys. Rev. B* **60**, 11005 (1999).
- [25] M. Korkusinski and P. Hawrylak, *Phys. Rev. B* **87**, 115310 (2013).
- [26] B. Larade and A. M. Bratkovsky, *Phys. Rev. B* **68**, 235305 (2003).
- [27] V. Janiš and J. Yan, *Phys. Rev. B* **103**, 235163 (2021).
- [28] P. Xue, *Phys. Rev. A* **81**, 052331 (2010).
- [29] G.-P. Guo, H. Zhang, T. Tu, and G.-C. Guo, *Phys. Rev. A* **75**, 050301(R) (2007).
- [30] A. N. Al-Ahmadi (2006), doi: [10.1021/acsenergylett.6b00569](https://doi.org/10.1021/acsenergylett.6b00569).
- [31] V. Moldoveanu and B. Tanatar, *Phys. Rev. B* **77**, 195302 (2008).
- [32] L. A. Agapito, N. Kioussis, and E. Kaxiras, *Phys. Rev. B* **82**, 201411(R) (2010).
- [33] S. Schröter, P.-A. Hervieux, G. Manfredi, J. Eiglsperger, and J. Madroñero, *Phys. Rev. B* **87**, 155413 (2013).
- [34] S. M. Reimann and M. Manninen, *Rev. Mod. Phys.* **74**, 1283 (2002).
- [35] L.-W. Wang and A. Zunger, *Phys. Rev. B* **59**, 15806 (1999).
- [36] G. Bester, *J. Phys.: Condens. Matter* **21**, 023202 (2008).
- [37] P. Matagne and J.-P. Leburton, *Phys. Rev. B* **65**, 155311 (2002).
- [38] D. V. Melnikov, P. Matagne, J.-P. Leburton, D. G. Austing, G. Yu, S. Tarucha, J. Fétig, and N. Sobh, *Phys. Rev. B* **72**, 085331 (2005).
- [39] M. Koskinen, M. Manninen, and S. M. Reimann, *Phys. Rev. Lett.* **79**, 1389 (1997).
- [40] M. Macucci, K. Hess, and G. J. Iafrate, *Phys. Rev. B* **55**, R4879 (1997).
- [41] M. Fujito, A. Natori, and H. Yasunaga, *Phys. Rev. B* **53**, 9952 (1996).
- [42] S. Bednarek, B. Szafran, and J. Adamowski, *Phys. Rev. B* **59**, 13036 (1999).
- [43] C. Yannouleas and U. Landman, *Phys. Rev. Lett.* **82**, 5325 (1999).
- [44] U. De Giovannini, F. Cavaliere, R. Cenni, M. Sassetti, and B. Kramer, *Phys. Rev. B* **77**, 035325 (2008).
- [45] B. Szafran, J. Adamowski, and S. Bednarek, *Phys. E* **5**, 185 (1999).
- [46] A. Emperador, E. Lipparini, and L. Serra, *Phys. Rev. B* **73**, 235341 (2006).
- [47] B. Reusch and H. Grabert, *Phys. Rev. B* **68**, 045309 (2003).
- [48] A. Puente, L. Serra, and V. Gudmundsson, *Phys. Rev. B* **64**, 235324 (2001).
- [49] R. M. Abolfath and P. Hawrylak, *J. Chem. Phys.* **125**, 034707 (2006).
- [50] Y. Nandan and M. S. Mehata, *Sci. Rep.* **9**, 2 (2019).
- [51] N. A. Bruce and P. A. Maksym, *Phys. Rev. B* **61**, 4718 (2000).
- [52] B. Szafran, S. Bednarek, and J. Adamowski, *Phys. Rev. B* **67**, 115323 (2003).
- [53] S. M. Reimann, M. Koskinen, and M. Manninen, *Phys. Rev. B* **62**, 8108 (2000).
- [54] S. A. Mikhailov, *Phys. Rev. B* **65**, 115312 (2002).
- [55] S. A. Mikhailov, *Phys. Rev. B* **66**, 153313 (2002).
- [56] M. Rontani, C. Cavazzoni, D. Bellucci, and G. Goldoni, *J. Chem. Phys.* **124**, 124102 (2006).
- [57] V. Popsueva, R. Nepstad, T. Birkeland, M. Førre, J. P. Hansen, E. Lindroth, and E. Waltersson, *Phys. Rev. B* **76**, 035303 (2007).
- [58] E. Waltersson, E. Lindroth, I. Pilskog, and J. P. Hansen, *Phys. Rev. B* **79**, 115318 (2009).
- [59] S. Kvaal, *Phys. Rev. B* **80**, 045321 (2009).
- [60] L. Sælen, E. Waltersson, J. P. Hansen, and E. Lindroth, *Phys. Rev. B* **81**, 033303 (2010).
- [61] S. A. Blundell and K. Joshi, *Phys. Rev. B* **81**, 115323 (2010).
- [62] T. Ezaki, N. Mori, and C. Hamaguchi, *Phys. Rev. B* **56**, 6428 (1997).
- [63] G. W. Bryant, *Phys. Rev. Lett.* **59**, 1140 (1987).
- [64] A. Harju, V. A. Sverdlov, R. M. Nieminen, and V. Halonen, *Phys. Rev. B* **59**, 5622 (1999).
- [65] A. Brataas, U. Hanke, and K. A. Chao, *Phys. Rev. B* **54**, 10736 (1996).
- [66] H. Saarikoski and A. Harju, *Phys. Rev. Lett.* **94**, 246803 (2005).
- [67] R. Egger, W. Häusler, C. H. Mak, and H. Grabert, *Phys. Rev. Lett.* **82**, 3320 (1999).
- [68] R. Egger, W. Häusler, C. H. Mak, and H. Grabert, *Phys. Rev. Lett.* **83**, 462(E) (1999).
- [69] F. Pederiva, C. J. Umrigar, and E. Lipparini, *Phys. Rev. B* **62**, 8120 (2000).
- [70] A. J. Williamson, J. C. Grossman, R. Q. Hood, A. Puzder, and G. Galli, *Phys. Rev. Lett.* **89**, 196803 (2002).
- [71] A. Ghosal, A. D. Güçlü, C. J. Umrigar, D. Ullmo, and H. U. Baranger, *Nat. Phys.* **2**, 336 (2006).
- [72] S. Weiss and R. Egger, *Phys. Rev. B* **72**, 245301 (2005).
- [73] L. Zeng, W. Geist, W. Y. Ruan, C. J. Umrigar, and M. Y. Chou, *Phys. Rev. B* **79**, 235334 (2009).

- [74] I. Kylänpää and E. Räsänen, *Phys. Rev. B* **96**, 205445 (2017).
- [75] M. Pedersen Lohne, G. Hagen, M. Hjorth-Jensen, S. Kvaal, and F. Pederiva, *Phys. Rev. B* **84**, 115302 (2011).
- [76] E. Waltersson, C. J. Wesslén, and E. Lindroth, *Phys. Rev. B* **87**, 035112 (2013).
- [77] R. J. Bartlett and M. Musiał, *Rev. Mod. Phys.* **79**, 291 (2007).
- [78] T. Gruber, K. Liao, T. Tsatsoulis, F. Hummel, and A. Grüneis, *Phys. Rev. X* **8**, 021043 (2018).
- [79] T. Schäfer, B. Ramberger, and G. Kresse, *J. Chem. Phys.* **148**, 064103 (2018).
- [80] T. Schäfer, N. Daelman, and N. López, *J. Phys. Chem. Lett.* **12**, 6277 (2021).
- [81] A. Grüneis, M. Marsman, and G. Kresse, *J. Chem. Phys.* **133**, 074107 (2010).
- [82] I. Heidari, N. Vaval, S. Pal, and D. G. Kanhere, *Chem. Phys. Lett.* **555**, 263 (2013).
- [83] C. Sloggett and O. P. Sushkov, *Phys. Rev. B* **71**, 235326 (2005).
- [84] E. Waltersson and E. Lindroth, *Phys. Rev. B* **76**, 045314 (2007).
- [85] I. Heidari, S. Pal, B. S. Pujari, and D. G. Kanhere, *J. Chem. Phys.* **127**, 114708 (2007).
- [86] J. F. Stanton and R. J. Bartlett, *J. Chem. Phys.* **98**, 7029 (1993).
- [87] A. I. Krylov, *Annu. Rev. Phys. Chem.* **59**, 433 (2008).
- [88] X. Wang and T. C. Berkelbach, *J. Chem. Theory Comput.* **16**, 3095 (2020).
- [89] A. Gallo, F. Hummel, A. Irmeler, and A. Grüneis, *J. Chem. Phys.* **154**, 064106 (2021).
- [90] B. T. G. Lau and T. C. Berkelbach, *J. Chem. Phys.* **152**, 224704 (2020).
- [91] T. M. Henderson, K. Runge, and R. J. Bartlett, *Phys. Rev. B* **67**, 045320 (2003).
- [92] M. Florian, C. Gies, F. Jahnke, H. A. M. Leymann, and J. Wiersig, *Phys. Rev. B* **87**, 165306 (2013).
- [93] Chr. Møller and M. S. Plesset, *Phys. Rev.* **46**, 618 (1934).
- [94] R. J. B. Isaiah Shavitt, *Many-Body Methods in Chemistry and Physics: MBPT and Coupled-Cluster Theory*, 1st ed., Cambridge Molecular Science (Cambridge University Press, Cambridge, 2009).
- [95] A. I. Krylov, *Acc. Chem. Res.* **39**, 83 (2006).
- [96] S. F. Boys, *Proc. R. Soc. London Ser. A* **200**, 542 (1950).
- [97] S. Obara and A. Saika, *J. Chem. Phys.* **84**, 3963 (1986).
- [98] R. Ahlrichs, *Phys. Chem. Chem. Phys.* **8**, 3072 (2006).
- [99] J. J. Shepherd, A. Grüneis, G. H. Booth, G. Kresse, and A. Alavi, *Phys. Rev. B* **86**, 035111 (2012).
- [100] M. Taut, *J. Phys.: Condens. Matter* **12**, 3689 (2000).